



ELSEVIER

July 2000

Materials Letters 49 (2001) 352–356

**MATERIALS
LETTERS**

www.elsevier.com/locate/matlet

Electron spectroscopic identification of carbon species on CN_x films

G. Soto *

Centro de Ciencias de la Materia Condensada, UNAM, Apdo. Postal 2681, 22800 Ensenada, B.C., Mexico

Received 25 October 2000; accepted 1 November 2000

Abstract

Carbon species produced during reactive laser deposition of carbon nitride (CN_x) films were characterized with Auger, X-ray photoelectron and electron energy-loss spectroscopies. The $\pi \rightarrow \pi^*$ and $\sigma + \pi$ plasmons show that the carbon atoms are in sp^2 configuration, and the absence of losses in the 26–30 eV is indicative of the non-existence of sp^3 -hybridized carbon. When the π loss is applied to N_{1s} or C_{1s} photoelectrons, the asymmetric tail in the XPS spectra is satisfactorily reproduced. With this analysis, the minor peaks are assigned to the inelastic losses, and the two main peaks to nitrogen, in substitution on sp^2 -hybridized carbon rings, developing pyridine and pyrrole-like configurations. © 2001 Elsevier Science B.V. All rights reserved.

PACS: 68.55Nq; 81.15Fg; 82.80.Pv

Keywords: Carbon nitride; CN_x ; Hybridization; Pyridine; Pyrrole; EELS; XPS

A large number of scientific reports dealt with the synthesis of carbon nitride (CN_x) solids. This experimental effort is driven by the conjecture, attributed to Cohen [1], that a solid formed by carbon and nitrogen would have a hardness comparable to that of diamond. Cohen's speculation was tested afterward using the known β - Si_3N_4 as an archetype structure by several ab initio calculations [2], giving the hypothetical β - C_3N_4 material. This material basically consists of sp^3 -hybridized carbon atoms bonded to sp^2 -hybridized nitrogen atoms [3]. In addition,

several CN_x structures have been theoretically proposed [4], resulting in two kinds of materials. Some of them are characterized by tetra-coordinated sp^3 -hybridized carbon, showing diamond-like properties (high atomic density, hardness, low electric and high thermal conductivity), while the others, characterized by graphite-like sp^2 -hybridized carbon, possess properties closer to that of graphite. Then, the distinction between sp^2 - and sp^3 -hybridized carbon is essential in the characterization of CN_x solids.

One of the most useful analytical tools for detecting differences in the hybridization character in pure carbon films is electron energy loss spectroscopy (EELS) [5]. This spectroscopy is based on the physical principle that electron, when traversing a thin foil of a material, may create various excitations by

* CCMC-UNAM, PO Box 439036, San Ysidro, CA 92143-9036, Mexico. Tel.: +52-6174-4603 ext. 408; fax: +52-6174-4604.

E-mail address: gerardo@ccmc.unam.mx (G. Soto).

transferring, or losing, energy to the material. One singularity of EELS among the electronic spectroscopies is that it probes the primary excitation, and for that reason, register each excitation event independently of the de-excitation mechanism. EELS is sensible to vibrational excitations (phonons), collective excitations (plasmons), intraband and interband transitions, and inner shell excitations. On carbon species, two main features have been observed in the reflection EELS. On one hand, we have the π plasmon [6]. Its physical origin is the dipole transition $\pi \rightarrow \pi^*$ between the π energy bands of carbon. This loss has been observed to appear near the edge of the backscattered electrons within a wide range of energies, and it is centered at 6 eV for HOPG [7]. However, this characteristic energy can be lower for other carbon systems, like polymers, fullerenes and aromatic compounds [8]. While the $\pi \rightarrow \pi^*$ transition is valid in the sp- or sp²-hybridized carbon, it is prohibited in the sp³. Therefore, it is representative of sp²- and sp-hybridized bonds. It is accepted as a rule that the lack of this π resonance would indicate the existence of a purely sp³-hybridized carbon bond [9]. On the other hand, we have the $\sigma + \pi$ peak. Making an allowance for the free electron approximation, then, the maximum in the energy-loss function correspond to the classical plasmons energy E_p :

$$E_p = \sqrt{4\pi\hbar^2 n_e e^2 / m_e}, \quad (1)$$

where n_e is the number of electrons taking part in plasmon oscillations per volume unit, m_e is the electron mass and e is the electron charge. This approximation is useful to estimate the plasmon energy for an unknown material, knowing the plasmon energy of a related isoelectronic and isomorphous material. For example, consider a crystalline silicon and diamond. Given that silicon and carbon contribute with the same number of valence band electrons, $\xi = 4$, we can write:

$$\frac{E_{p_{Si}}^2}{E_{p_{Diamond}}^2} = \frac{\frac{\xi}{V_{Si}}}{\frac{\xi}{V_{Diamond}}} = \frac{V_{Diamond}}{V_{Si}}, \quad (2)$$

where $V_{diamond}$ and V_{Si} are volumes that enclose the same number of atoms. Using the cell volumes, 160.15 and 45.385 Å³, for silicon and diamond, respectively, we can thus write that E_p (Diamond) \approx E_p (Si) * 1.88. The plasmon energy of crystalline silicon is 17 eV, and the estimated value with the above expression gives a 32.9 eV for diamond, compared to an experimental value of 33 eV [11]. In an analogous way, knowing the plasmon energy and cell dimensions for the β -Si₃N₄, the β -C₃N₄, plasmon energy can be estimated. The cell volume is 144.62 Å³ for β -Si₃N₄ [2] and its respective plasmon energy is in the 21.4–23.5 eV range [10]. By ab initio methods, the calculated equilibrium volume for β -C₃N₄ is 88.35 Å³ [2]. Then, the expected plasmon energy for β -C₃N₄ is: E_p (β -C₃N₄) \approx E_p (β -Si₃N₄) * 1.28. Thereafter, the probable plasmon energy for high-density carbon nitride material should be in the 27.5–30.0 eV range. Simplifying, for a two isoelectronic materials, the material with highest mass density must have a greater characteristic plasmon energy. Consequently, the search of any feature over 27 eV by EELS is good way to look for high-density carbon nitride solids.

Moreover, since the energy losses are independent of the origin of the electrons travelling in the solid, the photoelectrons should undergo the same process. Several works can be found where X-ray photoelectron spectroscopy (XPS) is used as central analytical technique to characterize CN_x films [12]. Although there is not an uncontroversial XPS assignment scheme for the principal contributions, there exists a tendency to interpret the asymmetric factor or peaks to the high binding-energy side, as chemical species on its own [12], without considering that the energy losses should necessarily be present.

With the aim to corroborate the preceding arguments, we have prepared a series of a-CN_x films by ablating a high purity graphite target, in the presence of molecular nitrogen under different experimental conditions. Laser energy, number of pulses and pulse repetition rate were kept fixed at 800 mJ, 10,000 and 10 Hz, respectively. This method has been proven to be useful for growing high-density hard films, as diamond-like carbon (DLC) [13] and related materials [14]. Then, the prepared material were in situ analyzed by XPS, Auger electron spectroscopy (AES), and EELS.

AES and XPS spectra show that the prepared films contain only carbon and nitrogen. Thus, we can unequivocally discard any C–O or N–O bonds. The maximum nitrogen concentration that was attainable with this preparation method was 30%. This corresponds to a stoichiometry of $CN_{0.42}$, in a good accord with the usual values reported utilizing PVD methods [15].

In Fig. 1, the EELS fingerprints are presented for: (a) graphite and (b) CN_x films grown at 100 mTorr of N_2 . The primary energy to collect those spectra is 1000 eV. This gives a mean free path of 27 Å; hence, the superficial effect are minimum and the observed transitions correspond to collective bulk excitations. The films grown at vacuum shows two main singularities, the $\sigma + \pi$ and π energy losses at an energy of 27 and 6 eV, respectively [16]. By means of the qualitative pattern matching suggested by Belton and Schmiege [5], it can be shown that the film is composed mainly of graphite-like sp^2 -hybridized carbon. For the films grown at 100 mTorr of nitrogen (Fig. 1(b)), the $\sigma + \pi$ peak is shifted down to 23 eV and the π peak is ill defined, estimated to be in the 3–5 eV region due to the wide background of inelastic backscattered electrons. The same pattern matching now gives films which are composed mostly of sp^2 -hybridized amorphous carbon network. By the reduction on the plasmon energy, we estimated a mass density loss of approximately 27 at.%

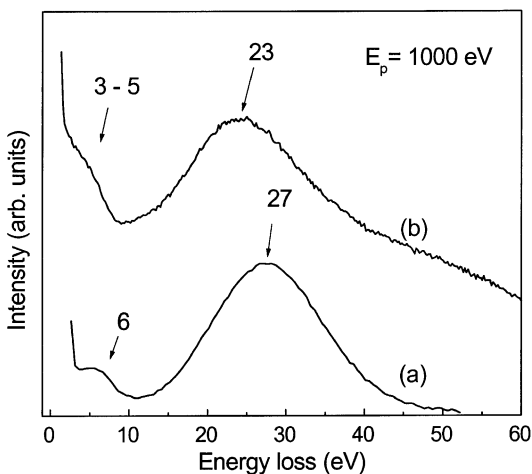


Fig. 1. EELS spectra for (a) graphite, (b) $CN_{0.42}$ film.

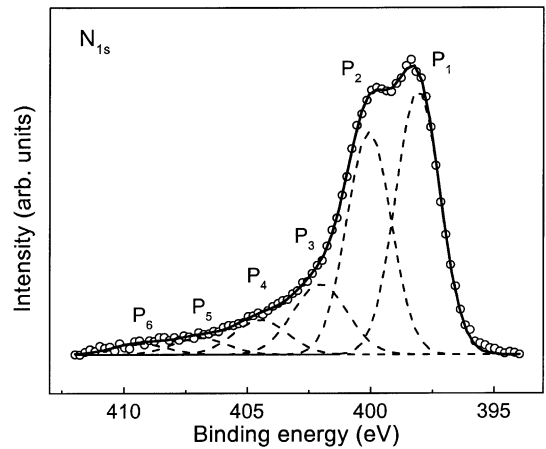


Fig. 2. High resolution XPS of N_{1s} for a sample prepared at 100 mTorr of N_2 .

for CN_x films, with respect to the vacuum-deposited graphite-like film. This is in a agreement with the conclusion of Spaeth et al. [17].

For a detailed analysis of XPS spectra, the electronic core levels of nitrogen and carbon were first background subtracted and then, numerically fitted to Gaussian functions. This is shown in Figs. 2 and 3 for N_{1s} and C_{1s} regions. The N_{1s} signal consists of two well resolved binding energy configurations, P_1 at 398.1 eV and P_2 at 400.1 eV. The numerical fitting shows that also for C_{1s} , two main contributions exists, Q_1 at 284.6 eV and Q_2 at 286.1 eV.

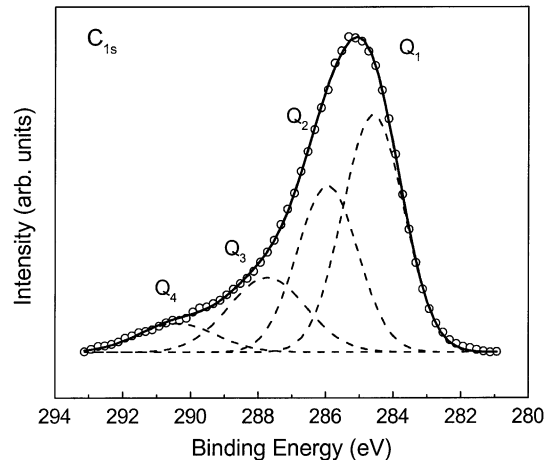


Fig. 3. High resolution XPS of C_{1s} for a sample prepared at 100 mTorr of N_2 .

These numerical values are in a good agreement with the reported values for N_{1s} and C_{1s} [12] and are tabulated in Tables 1 and 2, respectively. Taken in consideration that carbon atoms are mostly in the sp^2 configuration, according to the previous EELS data analysis, the main nitrogen and carbon chemical states must proceed from two or more different aromatic configurations. This will be discussed in more detail in a full paper, but we foresee that we agree with the interpretation of Spaeth et al. [17] and Peels et al. [18], who assign the most important contributions to pyridine and pyrrole-like configurations.

Focusing on the smaller N_{1s} contributions, P_3 at BE of 402.1 eV, this peak has been assigned to various bonding configurations: N–CO [19]; N–O [20]; N–N [21]. However, it has been observed in films containing no oxygen [9], as in our case here, indicating that P_3 could be related to a different cause. If P_1 photoelectrons suffer an energy loss due to π resonance, then a satellite peak should appear at the sum of P_1 and the corresponding energy loss (approximately 4 eV at it was determined by EELS). Subsequently, we assign the peak P_3 to a “shake up” line from P_1 peak. Similarly, peak P_4 may be associated to the corresponding energy loss of P_2 photoelectrons. The validity of this assignment could be reinforced, since the even smaller peaks, P_5 and P_6 , appearing at BE of about 8 eV above the main peaks, could be related to second-order losses. These succession of peaks cause the noticed asymmetry in the N_{1s} transition, as is evidenced in Fig. 1. In consistency with the analysis presented for the N_{1s} energy region, we assign peaks Q_3 and Q_4 in the C_{1s} region as resulting from the energy loss due to π excitation from the two main peaks Q_1 and Q_2 ,

Table 1
Gaussian fit to N_{1s}

Peak	Area (arb. units)	Center (eV)	Width (eV)	Height (arb. units)
P_1	39,000	398.1	1.8	17,290
P_2	34,000	400.1	1.8	15,070
P_3	10,190	402.1	2.2	4520
P_4	5850	404.2	2.2	2600
P_5	3260	406.3	2.2	1440
P_6	2280	408.8	2.2	1010

Table 2
Gaussian fit to C_{1s}

Peak	Area (arb. units)	Center (eV)	Width (eV)	Height (arb. units)
Q_1	62,630	284.6	1.8	27,760
Q_2	43,630	286.1	1.8	19,340
Q_3	16520	288.1	2.2	7320
Q_4	7980	290.4	2.2	3540

respectively. In Table 2, it can be verified that peak Q_3 is located at approximately 4 eV from peak Q_1 , and peak Q_4 at approximately 4 eV from peak Q_2 . With this analysis, the assignment of the smaller peaks to spurious chemical bonds is definitely unnecessary.

In summary, the presence of high-density carbon nitride phases should be evidenced by energy losses in the 26–30 eV range. Quite the opposite in our CN_x films, EELS do not show any feature over 26 eV, so we affirm the non-existence of sp^3 -hybridized carbon. Moreover, the existence of the π^* energy band, demonstrated by the $\pi \rightarrow \pi^*$ transition at 6 eV, and $\sigma + \pi$ plasmon at 23 eV are clear evidences of carbon in the more stable sp^2 configuration, with an electronic behavior similar to an amorphous carbon network. Thereafter, nitrogen adds in substitution on sp^2 -hybridized carbon rings. The two chemical states detected by XPS may well proceed from six- and five-member-rings. For that reason, we support the interpretation of Spaeth et al. [17] and Peels et al. [18], who assign the most important contributions to pyridine and pyrrole-like configurations. This reinforce the model suggested by Sjöström et al. [22] of a fullerene-like microstructure, where the connection between two sp^2 -hybridized CN_x layers are caused by buckling around pentagons, modified in a way that all C atoms are sp^2 -coordinated.

Acknowledgements

The technical assistance of Israel Gradilla, Wencel de la Cruz, Francisco Ruiz, Eloisa Aparicio and Margost Sainz are gratefully appreciated. The author is grateful for helpful discussions with L. Cota, E. Sámano, R. Machorro and M. Farías.

References

- [1] M.L. Cohen, *Phys. Rev. B* 32 (1985) 7988.
- [2] A.Y. Liu, M.L. Cohen, *Phys. Rev. B* 41 (1990) 10727.
- [3] A. Reyes-Serrato, D.H. Galván, I.L. Garzón, *Phys. Rev. B* 52 (1995) 6293.
- [4] P.H. Fang, *J. Mater. Sci. Lett.* 14 (1995) 536.
- [5] D.N. Belton, S.J. Schmieg, *J. Vac. Sci. Technol. A* 8 (1990) 2353.
- [6] N. Papageorgiou, M. Portail, J.M. Layet, *Surf. Sci.* 454–456 (2000) 462.
- [7] J.A. Martín-Gago, J. Fraxedas, S. Ferrer, F. Comin, *Surf. Sci. Lett.* 260 (1992) L17.
- [8] D.M. Poirier, J.H. Weaver, K. Kikuchi, Y. Achiba, *Z. Phys. D* 26 (1993) 79.
- [9] N. Hellgren, M.P. Johansson, E. Broitman, L. Hultman, J.-E. Sundgren, *Phys. Rev. B* 59 (1999) 5162.
- [10] V.A. Gritsenko, Yu.N. Morokov, Yu.N. Novikov, *Appl. Surf. Sci.* 113–114 (1997) 417.
- [11] M. Avalos-Borja, G.A. Hirata, O. Contreras, X.G. Ning, A. Duarte-Moller, A. Barna, *Diamond Relat. Mater.* 5 (1996) 1249.
- [12] C. Ronning, H. Feldermann, R. Merk, H. Hofsass, P. Reinke, J.-U. Thiele, *Phys. Rev. B* 58 (1999) 2207.
- [13] C.B. Collins, F. Davanloo, in: D.B. Chrisey, G.K. Hubler (Eds.), *Pulsed Laser Deposition of Thin Films*, Wiley, New York, 1994.
- [14] G. Soto, E.C. Sámano, R. Machorro, L. Cota, *J. Vac. Sci. Technol. A* 16 (1998) 1311.
- [15] S. Muhl, J.M. Mendez, *Diamond Relat. Mater.* 8 (1999) 1809.
- [16] F. Rossi, B. Andre, A. van Veen, P.E. Mijnders, H. Schut, F. Labohm, M.P. Delplancke, H. Dunlop, E. Anger, *Thin Solid Films* 253 (1994) 85.
- [17] C. Spaeth, M. Kuhn, F. Richter, U. Falke, M. Hietschold, R. Kilper, U. Kreissig, *Diamond Relat. Mater.* 7 (1998) 1727.
- [18] J.R. Pels, F. Kapteijn, J.A. Moulijn, Q. Zhu, K.M. Thomas, *Carbon* 33 (1995) 1641.
- [19] G.L. Chen, Y. Li, J. Lin, C.H.A. Huan, Y.P. Guo, *Surf. Interface Anal.* 28 (1999) 245.
- [20] W.T. Zheng, K.Z. Xing, N. Hellgren, M. Lögdlund, Å. Johansson, U. Gelivs, W.R. Salaneck, J.-E. Sundgren, *J. Electron Spectrosc. Relat. Phenom.* 87 (1997) 45.
- [21] A.K.M.S. Chowdhury, D.C. Cameron, M.S.J. Hashmi, *Surf. Coat. Technol.* 112 (1999) 133.
- [22] H. Sjöström, S. Stafström, M. Boman, J.-E. Sundgren, *Phys. Rev. Lett.* 75 (1996) 1336.